Konrad URBANSKI

Poznan University of Technology

Position estimation for PMSM drive equipped with the motor choke

Abstract. The paper presents results of studies on the sensorless drive with permanent magnet synchronous motor (PMSM) supplied through the motor choke. The position is estimated using a modified Luenberger observer. Its modification consists in using a PII^2 correction function instead a proportional one, which gives smaller estimation errors. The advantages of that observer structure are simple structure and the good performance of the drive despite the fact that the presence of the choke was not taken into account in the observer structure

Streszczenie. W artykule przedstawiono wyniki badań napędu bezczujnikowego z silnikiem synchronicznym o magnesach trwałych zasilanego poprzez dławik silnikowy. Wykorzystano zmodyfikowany obserwator Luenbergera. Modyfikacja polega na rozbudowie funkcji korekcji o dodatkowe integratory – co wpływa m.in. na zmniejszenie błędu odtwarzania położenia. Istotną cechą takiego obserwatora jest możliwość pracy napędu bez uwzględnienia w strukturze obserwatora obecności dławika w torze zasilania. (Odtwarzanie położenia w napędzie z PMSM zasilanego poprzez dławik silnikowy).

Keywords: sensorless control, PMSM, choke, observer.
Słowa kluczowe: sterowanie bezczujnikowe, SSMT, dławik, obserwator.

Introduction

Permanent Magnet Synchronous Motors (PMSM) are widely used in industrial drives. The main advantages are high power density, high torque-to- inertia ratio, small torque ripple and precise control at low speed range, possibility to torque control at zero speed, high efficiency and small size. To exploit presented advantages, a vector control should be used. Vector control allows the drive a good dynamic, effective performance especially during transients and prevents overload of the motor by controlling the torque. However, a motor shaft position sensor is required to enable the effective vector control of a PMSM. Eliminating the mechanical sensor which is used to measure and calculate the shaft position and its speed is subject of the research, which is currently developed in various research centers [1]–[4], which are based on back EMF estimation, Kalman filter or using neural network. The other way is to use a MRAS based estimator [5], mainly used with induction motors [6], however, the observer may be used also with SRM [7] and PMSM [8] based drive. The sensor elimination allows increase of reliability and decreasing costs for the drive.

The paper presents the concept and the results of the control algorithm in simulation and experimental tests for the PMSM powered by the PWM inverter. The motor is supplied using choke which gives possibility to extend the lifespan of the motor which is working in hard conditions, e.g. when it is connected to the inverter by long wires. This is achieved mainly by reducing the dv/dt and smoothing the current waveforms.

An additional feature of the choke is to limit short-circuit currents and reduction the insulation problems and the emissions. The use of the choke is recommended in the following cases:
- the long cables between inverter and motor
- high switching frequency
- compliance the EMC requirements

PMSM drive

Used in the paper the control structure is presented in Figure 1. It presents a well-known vector control system. The drive is equipped with cascade control structure using closed speed control loop with inner currents control loop. The motor is fed by the PWM inverter working with six pulse rectifier. The control system includes vector control system of stator currents in *dq* independent axes - controllers R_{iq} (1) and R_{id} (2), speed controller R_{ω} (3) and position observer (4). The system is equipped with position and speed sensors which are used only to analysis of the estimation quality. The estimated value of the actual shaft position is used in transforming blocks of the coordinate system *dq-αβ* and *αβ-dq*. The estimated value of the speed is used in control loop of the speed. The presented structure gives a possibility to test system in closed mode (observed values are used to control drive) and open mode (observed values are only considered) using manual switches as it is shown in Figure 1.
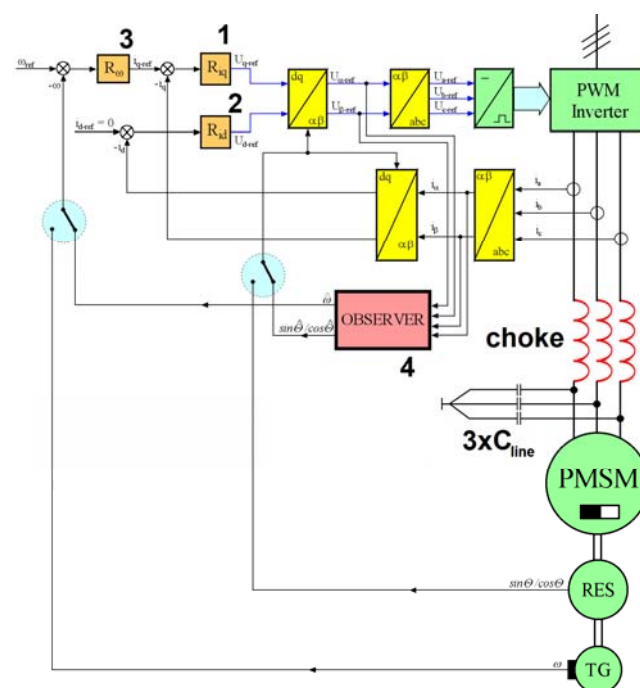

Fig.1. The sensorless drive control structure

Such control mode switches are implemented both in simulation model and real system. To achieve smooth observed values, a reference voltage is used instead of measured ones. Usage of the reference voltage value in the estimation algorithm significantly facilitates calculations and affects on the quality of the values obtained during shaft position calculations. The quality was defined as the low

value and the small oscillations of the position error. The present aim is to check the correct operation of the sensorless algorithm for the case when all measuring elements are located before the motor choke. A simplified mathematical model of synchronous motor with permanent magnets was adopted for the study. It is assumed that the rotor has no windings, eddy currents and the effect of temperature is neglected, produced by the rotor the flux is constant [9].

Back EMF observer

A simple and effective structure of an observer is proposed in this paper. The observation idea is based on the back EMF estimation. The method based on modified Luenberger observer [10] is a very useful tool in sensorless PMSM drive equipped with the motor choke. The observer is based on using a motor model described only by the two first electrical PMSM equations in stationary coordinates system $\alpha\beta$, with state variables - current components i_α, i_β, input variables - voltages v_α, v_β and back EMF e_α, e_β considered as disturbances [11].

However, this simple structure requires the change of the observer parameters settings depending on the operating point. The *gain scheduling* method should be used. Its proper change is very important in the case where the speed range is wide.

One can write the extended state formulas in a matrix form as below:

$$(1) \qquad \dot{\hat{\mathbf{x}}}_{\mathbf{E}} = \mathbf{A}_{\mathbf{E}}\hat{\mathbf{x}}_{\mathbf{E}} + \mathbf{B}_{\mathbf{E}}\mathbf{u} + \mathbf{K}[\Delta\mathbf{i}]$$

$$(2) \qquad \mathbf{x}_E = \begin{bmatrix} i_\alpha, i_\beta, e_\alpha, e_\beta \end{bmatrix}^T$$

Here the index „*E*" means - *extended*. In this way, a matrix corrector of a proportional gains **K** is obtained, or in a more general form, where the form of the corrector can be described by the error function **F[Δi]:**

$$(3) \qquad \dot{\hat{\mathbf{x}}}_{\mathbf{E}} = \mathbf{A}_{\mathbf{E}}\hat{\mathbf{x}}_{\mathbf{E}} + \mathbf{B}_{\mathbf{E}}\mathbf{u} + \mathbf{F}[\Delta\mathbf{i}]$$

In order to increase the accuracy of observation especially in dynamic states or in high-step calculations, the structure of the corrector can be expanded by adding another integrator, to give correction function „PII²" [12]:

(4)
$$\mathbf{F}\left[\Delta\mathbf{i}\right] = \mathbf{K}_p\left[\Delta\mathbf{i}\right] + \mathbf{K}_i\int\left[\Delta\mathbf{i}\right]\mathbf{dt} + \mathbf{K}_{i2}\int\left[\int\left[\Delta\mathbf{i}\right]\mathbf{dt}\right]\mathbf{dt}$$

Thus the observer equations take the following form:

$$\frac{d\hat{i}_\alpha}{dt} = -\frac{R}{L}\hat{i}_\alpha - \frac{1}{L}\hat{e}_\alpha + \frac{1}{L}v_\alpha + F_{i\alpha}(\hat{i}_\alpha - i_\alpha)$$

$$\frac{d\hat{i}_\beta}{dt} = -\frac{R}{L}\hat{i}_\beta - \frac{1}{L}\hat{e}_\beta + \frac{1}{L}v_\beta + F_{i\beta}(\hat{i}_\beta - i_\beta)$$

$$(5) \qquad \frac{d\hat{e}_\alpha}{dt} = F_{e\alpha}(\hat{i}_\alpha - i_\alpha)$$

$$\frac{d\hat{e}_\beta}{dt} = F_{e\beta}(\hat{i}_\beta - i_\beta)$$

where F_{xy} are the correction function, independently for back EMF and current estimation. Observer in axes α and β has the same parameters. So, the observer contains of six independent parameters.

Simulation tests have confirmed the advantages of an observer of this structure manifested in above conditions. Calculation of the velocity and position determination is made on the basis of estimated back EMF in the coordinate system $\alpha\beta$.

$$(6) \qquad \sin\hat{\Theta} = -\frac{\hat{e}_\alpha}{|\hat{e}|} \qquad\qquad \cos\hat{\Theta} = \frac{\hat{e}_\beta}{|\hat{e}|}$$

where

$$(7) \qquad |\hat{e}| = k_{SEM} \cdot \sqrt{\hat{e}_\alpha^2 + \hat{e}_\beta^2}$$

and k_{SEM} is a scale factor.

The speed can be determined from that equation:

$$(8) \qquad |\hat{\omega}| = \frac{|\hat{e}|}{k_e}$$

In a case of the back EMF estimation using high-step calculations, the calculation of speed using position derivative, enforces a strong filtering of the signal. It is caused by ripples in the estimated position waveforms. As a result, a large value of the delay in the speed feedback loop is present, which significantly reduces the dynamics of the drive. The method based on equations (6-8) allows the drive to maintain a satisfactory dynamics, but the price for this is lack of information about the speed sign. The scheme of the whole observer system is presented in Figure 2. The observer parameters were chosen using method RWC (random weight change) [12], where the method was originally applied to learning the artificial neural networks [13].
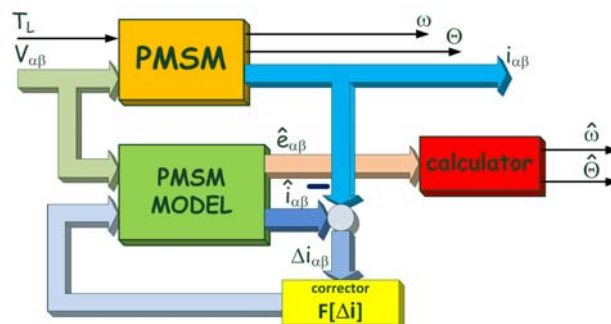

Fig.2. General structure of the back EMF observer including position and speed calculator

Simulation research

The presented objects have been modeled in MATLAB-Simulink environment. The model uses accurate circumferential model of the power system (inverter, choke), however, the motor was modeled with ordinary simplifying assumptions such as constant resistance and inductance in stator windings, symmetry of windings, and isotropic properties of motor. This model takes into account the dead time phenomenon. The used method is based on implementation of dead time inside inverter driver. The motor model was calculated with small sampling step 0.1 µs or 1 µs, the speed controller, the observer and the calculator were sampled with a step of 100 µs. The lower values of the sampling times have proved the correctness of the concept, while the bigger value was used during simulation to speed-up calculations. The presented waveforms are prepared using 100 µs calculation step, the same value as is used in the DSP based control system at laboratory stand. Presented system was examined in closed loop mode: all signals produced by the observer were used in the control loop and the measured and estimated signals were used only to calculate the quality of

estimation but the sensorless mode was switched on after artificial start-up procedure. Selected waveforms are shown.
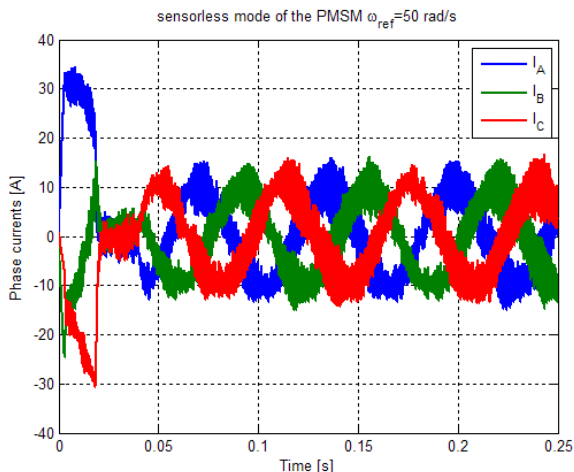

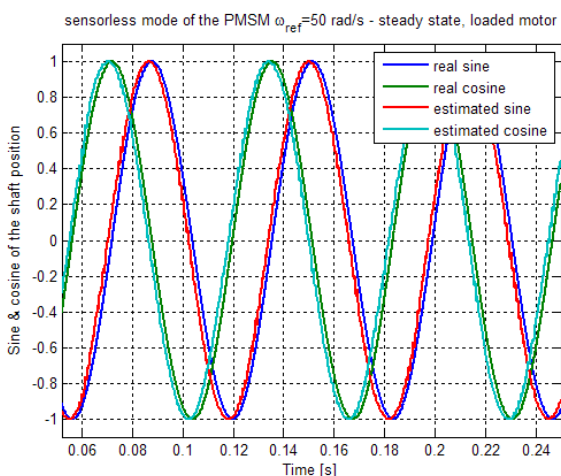Fig.3. Waveforms of the real phase currents during the test

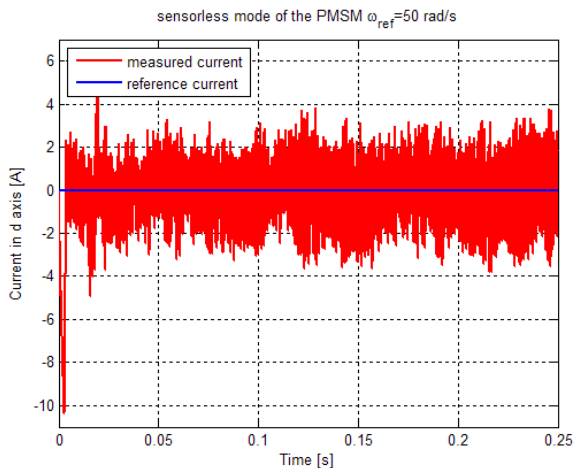Fig.4. Waveforms of the real and estimated sine and cosine at the steady state

Fig.5. Waveforms of the measured and reference *d* axis currents at the steady state– sensorless mode

The test procedure consists of start-up from standstill to the speed of 50 rad/s, then in time t=40 ms there is the load step change into nominal value. The inverter model takes into account the phenomenon of the dead time. The measurement noise is also taken into account through addition of the random signal into "measured" currents. Figure 3 shows real phase currents during the test. In Figure 4 the waveforms of the calculated sine and cosine which are used in the axes conversion blocks are shown.

Figures 5 and 6 prove the performance of the observer: waveforms of the estimated currents are quite near the reference currents. The roughness is caused by the inverter operation, relatively large calculation step and the dead time phenomenon. The roughness is also visible in sensor mode (Fig. 7). Figure 8 presents waveforms of the calculated and real position: the estimation accuracy is right. The median of the absolute value of the position error in the steady state is equal 0.82 °. Finally, Figure 9 presents waveforms of back EMFs: the real and estimated ones.
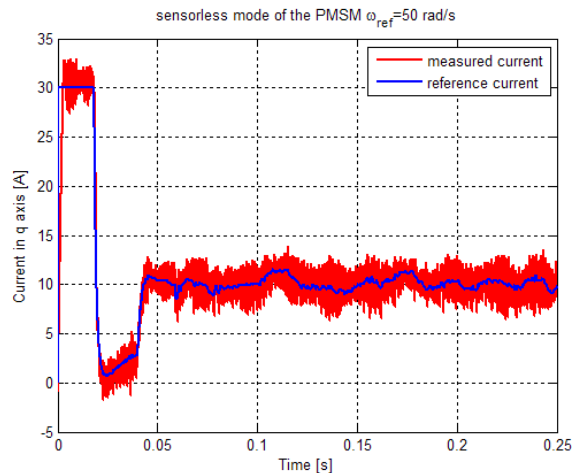

Fig.6. Waveforms of the measured and reference *q* axis currents during the test – sensorless mode
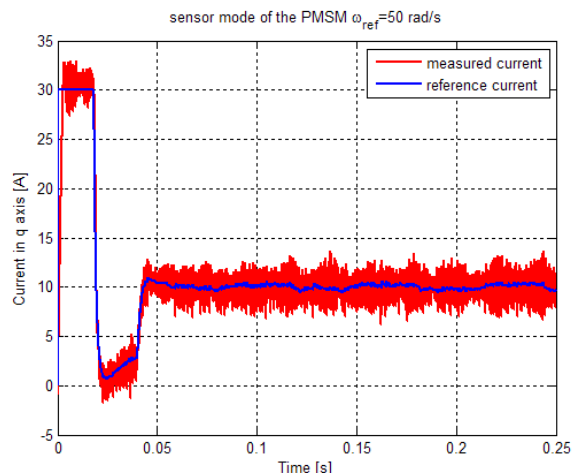

Fig.7. Waveforms of the measured and reference *q* axis currents during the test – sensor mode
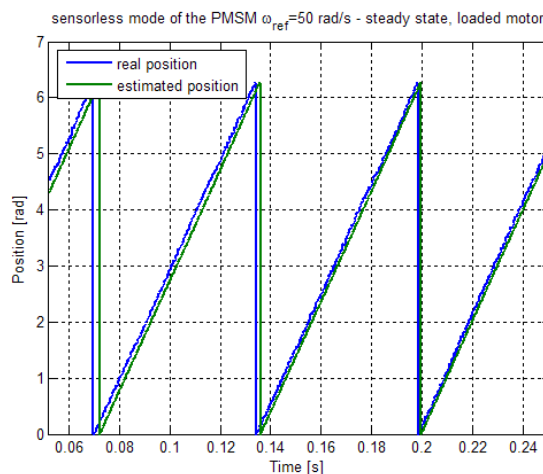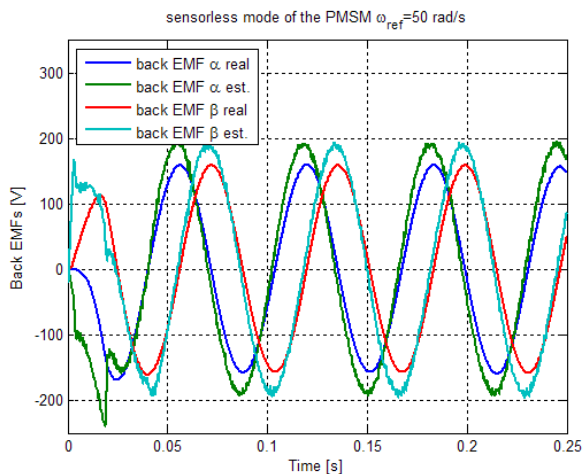

Fig.8. Waveforms of the real and estimated position

Fig.9. Waveforms of the "real" and estimated α and β back EMFs during the test – sensorless mode

One can notice that the initial estimation error is high due to improper observer parameters set for low speed range. Then, after reaching the speed, for which the parameters were chosen, the error value decreases. The phase shift is reduced and only gain inaccurate value is noticeable. The gain inaccuracy is compensated using gain scheduling method. Amplitude inaccuracy is negligible importance. It is more important the accuracy of back EMF phase estimation, because it directly affects the position estimation error.

Experimental results
After achieving stable sensorless work of simulation drive model, in order to confirm the concept, the laboratory tests were performed. The test bench consists of PMSM, laboratory inverter controlled by means of microprocessor system with floating point DSP from SHARC family based on evaluation board, a resolver (used only for comparison purpose), current and voltage sensors and measurements interfaces. Motor is supplied by three-phase voltage source inverter through three one phase chokes. Inverter is working at 10 kHz PWM frequencies. The observer with PII^2 correction was used in laboratory experiment. The observer algorithms as well as control algorithms were implemented on DSP processor. The measurement algorithms are implemented in additional FPGA evaluation board.
Parameters of the motor:

Type: Control Techniques 095U2B300BASAA100190
Rated power: 1.23 kW
Nominal speed: 3000 rpm
Rated torque: 3.9 Nm
measured resistance: 2 Ω
measured inductance: 5.7 mH
total moment of inertia: 24.96 kg·cm^2

Choke parameters:
measured resistance: 0.45 Ω
measured inductance: 5.7 mH

All the waveforms were obtained in steady state in closed loop mode, where all estimated signals were used in control chain. The reference speed is equal to 50 rad/s and the motor is unloaded. Selected results are presented below. Figure 10 presents sensorless performance of the drive. The channel 2 is the measured position. This waveform proves the stable and smooth work of the drive.
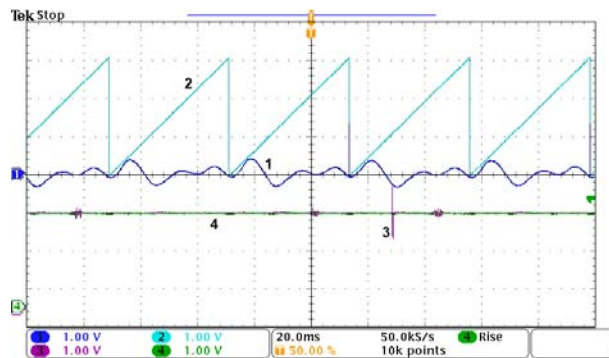

Fig.10. Sensorless mode, reference speed: 50 rad/s, steady state, unloaded. CH1: position estimation error multiplied by 10, CH2: measured position, CH3: measured speed, CH4: estimated speed
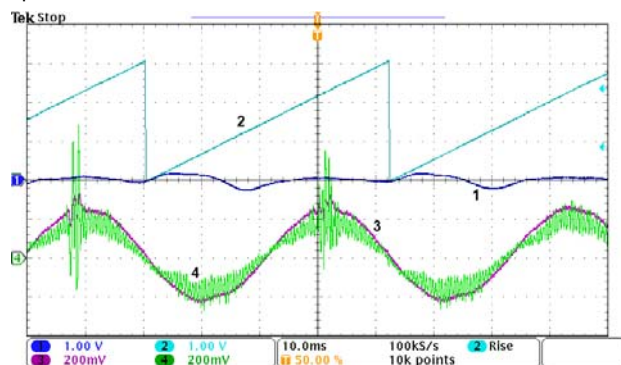

Fig.11. Sensor mode, reference speed: 50 rad/s, steady state, unloaded. CH1: position estimation error multiplied by 10, CH2: measured position, CH3: measured current i_α, CH4: estimated current i_α
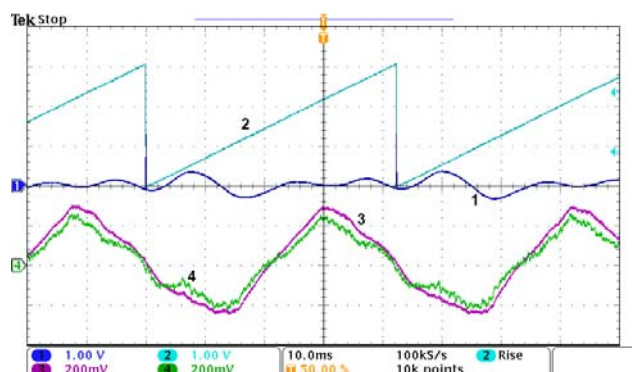

Fig.12. Sensorless mode, reference speed: 50 rad/s, steady state, unloaded. CH1: position estimation error multiplied by 10, CH2: measured position, CH3: measured current i_α, CH4: estimated current i_α
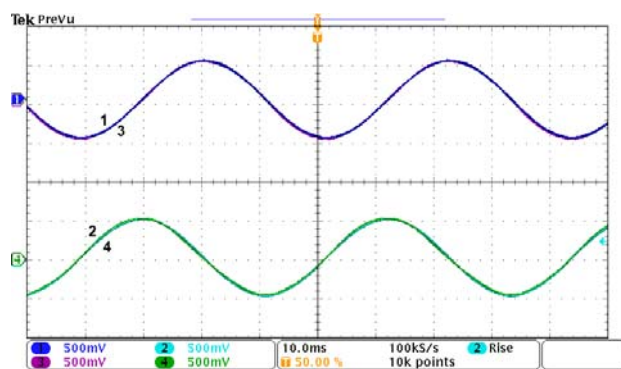

Fig.13. Sensorless mode, reference speed: 50 rad/s, steady state, unloaded. CH1: sine of the measured position, CH2: cosine of the measured position, CH3: sine of the estimated position, CH4: cosine of the estimated position

Channel 1 is the position estimation error multiplied by 10 (so, the scale for channel 1 is 12 degree per division). The position estimation error waveform reaches the maximum value of 4.8 ° for the motor's first poles pair only. For the other two poles pairs the error is significantly smaller. Its mean square error for one rotation is about 1.2 °. The important advantage of that observer corrector structure consists in a possibility to decrease the constant part of the error. It is achieved by proper modifying of the integral and double integral signal course gains in observer. The channel 3 and 4 presents the measured and estimated speed, respectively. The estimated speed is smooth and what is documented by stable speed waveform (there are only visible distortions in oscilloscope/registration side, without affecting the operation of the drive). Figure 11 and 12 show the currents in α axis in the stationary coordinate system in sensor mode and sensorless mode of operation, respectively. In both figures, the currents are measured in the channel 3 and estimated in channel 4. To synchronize the waveform, the channels 1 and 2 show the same signals as in Figure 10, respectively. The current controller has the same parameters set. Finally, the Figure 13 shows the sine and cosine of the shaft position. Those variables are used to convert between different coordinate systems. A good agreement of the respective waveforms is shown.

Conclusion

In the paper it was proved that modified Luenberger structure (PII²) gives possibility to perform sensorless mode of operating with PMSM even with motor powered through the choke. The simulation and experiments show that, in a case when a choke is used in the motor supply lines, it not excludes the use of the drive without mechanical sensors. Moreover, if the inductance value is comparable as that in the motor, the sensorless drive still can work properly.

The presented observer structure may be simple implemented in DSP. Such structure of observer, which uses the PII² corrector, has very important advantage: it gives a possibility to decrease considerably the constant error component. To find the suitable observer parameter set is possible to use the simple RWC algorithm presented in [12]. However, the fastest method is to use modified method, presented in [14] - where multi-stage searching of parameters is used. Those higher stages are performed by proper modifying the integral and double integral values for observer parameters.

The main advantage of that structure consists in a good performance of the drive despite of the fact that the presence of the choke was not taken into account in observer structure.

REFERENCES

[1] A. Accetta, M. Cirrincione, and M. Pucci, TLS EXIN based neural sensorless control of a high dynamic PMSM, *Control Engineering Practice*, Apr. 2012.

[2] T.-F. Chan, P. Borsje, and W. Wang, Application of Unscented Kalman filter to sensorless permanent-magnet synchronous motor drive, presented at the Electric Machines and Drives Conference, IEMDC, 2009, pp. 631–638.

[3] F. Genduso, R. Miceli, C. Rando, and G. R. Galluzzo, Back EMF Sensorless-Control Algorithm for High-Dynamic Performance PMSM, *IEEE Transactions on Industrial Electronics*, vol. 57, no. 6, pp. 2092–2100, Jun. 2010.

[4] K. Urbanski, Sensorless control of PMSM high dynamic drive at low speed range, in *2011 IEEE International Symposium on Industrial Electronics (ISIE)*, 2011, pp. 728–732.

[5] J. van Amerongen, MRAS: Model Reference Adaptive Systems, *Journal A*, vol. 22, no. 4, pp. 192–198, 1981.

[6] P. P. Cruz and J. J. Rodriguez Rivas, Induction motor space vector control using adaptive reference model direct and indirect methods, in *Industrial Electronics, 2000. ISIE 2000. Proceedings of the 2000 IEEE International Symposium on*, 2000, vol. 1, pp. 300–305.

[7] K. Urbanski, Sensorless control of SRM at medium speed range, *Archives of Electrical Engineering*, vol. 60, no. 2, pp. 179–185, Czerwiec 2011.

[8] Y. S. Kim, S. K. Kim, and Y. A. Kwon, MRAS based sensorless control of permanent magnet synchronous motor, presented at the SICE Annual Conference, Fukui, 2003.

[9] P. Vas, *Sensorless Vector and Direct Torque Control*. Oxford ; New York: Oxford University Press, 1998.

[10] D. Luenberger, An introduction to observers, *IEEE Transactions on Automatic Control*, vol. 16, no. 6, pp. 596–602, Dec. 1971.

[11] F. Parasiliti, R. Petrella, and M. Tursini, Sensorless speed control of a PM synchronous motor by sliding mode observer, in *Industrial Electronics, 1997. ISIE'97., Proceedings of the IEEE International Symposium on*, 1997, pp. 1106–1111.

[12] K. Urbanski and K. Zawirski, Adaptive observer of rotor speed and position for PMSM sensorless control system, *COMPEL: Int J for Computation and Maths. in Electrical and Electronic Eng.*, vol. 23, no. 4, pp. 1129–1145, 2004.

[13] B. Burton, F. Kamran, R. G. Harley, T. G. Habetler, M. A. Brooke, and R. Poddar, Identification and control of induction motor stator currents using fast on-line random training of a neural network, *IEEE Transactions on Industry Applications*, vol. 33, no. 3, pp. 697–704, Jun. 1997.

[14] K. Urbanski, Sensorless control of the PMSM drive equipped with hysteresis band current controller, in *X Krajowa Konferencja Naukowa Sterowanie w Energoelektronice i Napędzie Elektrycznym, SENE 2011*, Łódź, Poland, 2011.

Author: Konrad Urbanski, Poznan University of Technology, Institute of Control and Information Engineering, ul. Piotrowo 3a, 60-965 Poznan, Poland, E-mail: konrad.urbanski@put.poznan.pl